IJCRT.ORG ISSN : 2320-2882

INTERNATIONAL JOURNAL OF CREATIVE RESEARCH THOUGHTS (IJCRT)

An International Open Access, Peer-reviewed, Refereed Journal

A Regenerative Electromechanical Vehicle Propelled By The Kinetic Energy Harnessed From The Rotational Motion Of Its Wheels.

Kishore M P
Assistant professor
Department of EEE
Vidya Vikas Institute of Engineering and Technology,Mysore

Sanjana H M
Student
Department of EEE
Vidya Vikas Institute of Engineering and Technology,Mysore

Akshitha Y P
Student
Department of EEE
Vidya Vikas Institute of Engineering and Technology,Mysore

Rakshitha P
Student
Department of EEE
Vidya Vikas Institute of Engineering and Technology,Mysore

C S Devika
Student
Department of EEE
Vidya Vikas Institute of Engineering and Technology,Mysore

***Abstract*—**Research into energy collecting technology has grown significantly in recent years as a result of the growing demand for alternate energy sources. Different technologies have been developed recently, and the specific issue of energy harvesting on road pavements is a very young area of research.

None of them, however, has demonstrated both high conversion efficiency and technical and financial feasibility. In order to transfer energy from the device surface to an electrical generator, this study discusses the construction of a new mechanical system to be used on an electromechanical device that harvests energy from road pavement. The major objective is to measure and contrast the new system's energy harvesting, transmission, and conversion efficiency with existing systems. There are offered conclusions about the effectiveness of the system.

Keywords: Road pavement; Energy Harvesting; Energy conversion; System modelling.

I. INTRODUCTION

With the current energetic paradigm, the majority of electrical energy production involves the combustion of fossil fuels, which results in high fuel prices for economies and irreparable environmental harm [1]. Over 80% of energy production in 2014, according to the International Energy Agency [2], came from fossil fuels. Since most electrical energy is currently produced outside of cities, using non-renewable resources and resulting in energy losses between the site of production and the point of consumption, immediate action is needed to change the paradigm of electrical energy generation. Energy harvesting is defined as a concept in which energy is obtained from multiple sources, transformed, stored, and used while utilizing interfaces, storage units, and other components [3], [4]. Simply said, energy harvesting is the process of transforming ambient energy—the energy that is

already present in the environment—into other usable forms of energy, such, for instance, electrical energy [5].

Macro energy harvesting sources, which are primarily linked to solar, wind, hydro, and ocean energy, are divided into two categories: micro energy harvesting sources, which are primarily linked to electromagnetic, electrostatic, heat, thermal variations, mechanical vibrations, acoustic, and human body motion [3], [6], [7]. Large-scale energy harvesting, which typically involves kJ or more, is connected to macro energy harvesting.

Small-scale energy harvesting, often of the order of a J or less, is related to micro energy harvesting. Vehicle loads continuously impact road surfaces. From this energy can be extracted and, with the right technologies, converted into electrical energy. [8], [9]. Energy is used by engines in vehicles, and energy is released in various ways by various components. The road pavement absorbs some of the energy that automobiles emit into the air. The vehicle's wheels receive anywhere between 15% and 21% of the energy [10], [11] Because there are so many vehicles in developed country cities, a significant amount of energy is wasted on the surface of the roads. So here is a device that capture and transform mechanical energy from vehicles into electrical energy.

Additionally, for the majority of the technologies currently in use, no system modeling or computational simulations have been published to allow for the analysis of energy harvesting, transmission, and conversion efficiency. This analysis would allow for the determination of their overall efficiency and the drawing of conclusions regarding their viability.

To transmit the energy received by the RPEH device surface into an electromagnetic generator, which will be modeled and simulated in the current study in order to determine its efficacy, a novel mechanical system to be implemented on an electromechanical device will be proposed. The efficiency of the proposed technologies will be compared.

II. VEHICLE-ROAD INTERACTION

A. Vehicle released energy

For the past 50 years, models of four-wheeled vehicles have been studied. For several applications, including the investigation of vehicle vibrations, validated models have been created based on well-understood dynamics and properties [12]–[17]. The bicycle-car model, which is shown in Fig. 1, is the best vehicle model to use for simulating a vehicle and researching its interaction with a road pavement energy harvesting device that causes vibrations on the vehicle chassis and typically includes a moveable surface. This model contains the front and rear suspension systems, front and rear tires, the vehicle's sprung mass (ms), which is equal to half of the vehicle's mass, the rear unsprung mass (msf), the front and rear unsprung mass (muf), and a pavement surface with a one-degree vertical displacement.

The parameters Ks, Cs, Kt, and Iy stand in for the suspension stiffness, suspension damping, tire stiffness, and vehicle body inertia, respectively. In terms of motion coordinates, xs stand for the vehicle's sprung mass, xur for its unsprung rear mass, xuf for its unsprung front mass, and v for its unsprung pitch.

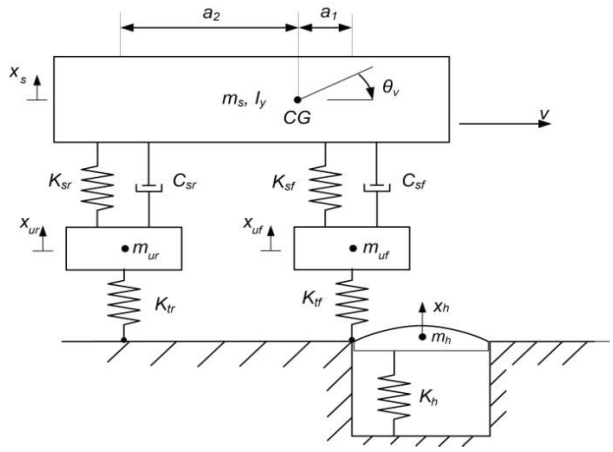

Fig. 1 Bicycle-car model with a movable surface applied on the pavement.

The governing differential equations of motion for this model are presented by (1-4), with (5) presenting the governing differential equation of the RPEH device surface.

$$m_s\ddot{x}_s + C_{sf}(\dot{x}_s - \dot{x}_{uf} - a_1\dot{\theta}_v) + C_{sr}(\dot{x}_s - \dot{x}_{ur} + a_2\dot{\theta}_v) + K_{sf}(x_s - x_{uf} - a_1\theta_v) + K_{sr}(x_s - x_{ur} + a_2\theta_v) = 0 \quad (1)$$

$$I_y\ddot{\theta}_v - a_1C_{sf}(\dot{x}_s - \dot{x}_{uf} - a_1\dot{\theta}_v) + a_2C_{sr}(\dot{x}_s - \dot{x}_{ur} + a_2\dot{\theta}_v) + a_1K_{sf}(x_s - x_{uf} - a_1\theta_v) + a_2K_{sr}(x_s - x_{ur} + a_2\theta_v) = 0 \quad (2)$$

$$m_{uf}\ddot{x}_{uf} - C_{sf}(\dot{x}_s - \dot{x}_{uf} - a_1\dot{\theta}_v) + K_{tf}(x_{uf} - x_h) - K_{sf}(x_s - x_{uf} - a_1\theta_v) = 0 \quad (3)$$

$$m_{ur}\ddot{x}_{ur} - C_{sr}(\dot{x}_s - \dot{x}_{ur} + a_2\dot{\theta}_v) + K_{tr}(x_{ur} - x_h) - K_{sr}(x_s - x_{ur} + a_2\theta_v) = 0 \quad (4)$$

$$m_h\ddot{x}_h - K_{tf}(x_{uf} - x_h) - K_{tr}(x_{ur} - x_h) + K_hx_h = 0 \quad (5)$$

The longitudinal component of the force is precisely proportional to vehicle acceleration (6). Therefore, (7) gives the variation of the vehicle's acceleration, and (8) calculates the vehicle's speed (v). It is possible to calculate the vehicle's acceleration and afterwards its speed at each iteration (index i) using the longitudinal forces. The same holds true for the location of the car, which is indicated.

$$\sum F_x = m_v a \quad (6)$$

$$\partial a = \partial \sum F_x/m_v \quad (7)$$

$$v_i = v_{i-1} + a\,\Delta t \quad (8)$$

$$x_i = x_{i-1} + v_{i-1}\,\Delta t + \frac{1}{2}a_i\,\Delta t^2 \quad (9)$$

The reduction in vehicle speed, which is connected to the loss of kinetic energy, can be used to calculate the energy released from the vehicle using equation (10).

$$\partial E_v = \frac{1}{2}m_v\,\partial(v^2) \quad (10)$$

B. RPEH device surface

RPEH devices have a surface displacement, whereas standard speed reducer equipment (SRE) does not. SRE can also have varying surface geometries and dimensions. The initial and ultimate height at the road's pavement level is the same, nevertheless, so that the vehicle wheel makes contact with the equipment at both points at this height. In order for the vehicle's tire to immediately reach the pavement level after it loses contact with the SRE surface, the final height of RPEH devices should not be the same as their initial height because their surface has a vertical displacement and moves downward with the force applied by the moving vehicle wheel. length of the surface and h max, which stands for the surface profile's maximum height.

The surface profile height ought to match the surface maximum displacement at the surfaces' maximum length. A particular surface profile known as Crest was taken into consideration to achieve this significant feature (Fig. 2).

This surface profile equation is given by (11), where z denotes the surface's vertical position, x denotes its longitudinal position, l max denotes the surface's maximum length, and h max denotes the surface profile's maximum height.

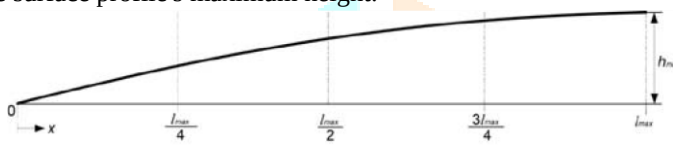

Fig. 2 *Crest* surface profile for a one degree of freedom movable surface

$$z(x) = \sqrt{\left[1 - \frac{(x - l_{max})^2}{(l_{max})^2}\right](h_{max})^2} \qquad (11)$$

C. Energy harvested

In the case of a movable surface with one degree of freedom, the energy associated with the surface motion (EHa) is computed by taking into account the total force applied to the surface (Fz) and the velocity of the surface. Using (12), compute the surface displacement (xh). We can use Equation (13) to Estimate the energy harvesting process's efficiency (Ha), Computing the difference between the vehicle's energy loss (Ev) and the energy captured by the equipment's surface.

$$\partial E_{Ha} = F_z \, \partial x_h \qquad (12)$$

$$\eta_{Ha} = E_{Ha}/E_v \qquad (13)$$

III. RPEH ELECTROMECHANICAL SYSTEM DEVELOPMENT

A. Introduction

Different methods can be employed to transfer the captured energy from the surface of a Resonant Piezoelectric Energy Harvester (RPEH) to an electric generator. According to a prior study [9], it can be deduced that the majority of existing RPEH devices operate on electromechanical principles and incorporate mechanical systems to translate surface movement into electrical energy via electromagnetic generators.

For the purpose of achieving rotational motion as an output, two primary systems are commonly adopted: the rack and pinion system, and the lever system.

The most fundamental mechanical approach for transforming linear surface motion into rotational motion of a shaft is executed through the rack and pinion system. In this configuration, the rack is typically directly linked to the surface, while the pinion makes contact with the rack and is connected to a shaft. This shaft then sets the electric generator in motion. Frequently, the generator shaft is associated with an inertia wheel (IW), and the pinion is fastened to the shaft using a unidirectional bearing, also referred to as a clutch bearing. This system incorporates a spring that restores the surface to its initial position. The efficiency of these systems in terms of conversion can achieve levels of up to 40% [9].

An alternative mechanical method frequently utilized for converting linear surface motion into rotational motion of a shaft is the lever system. Although this system has the advantage of amplifying surface movement, it accompanies a trade-off involving force loss. In its application within an energy harvesting device, a bar, directly connected to the surface, activates a lever at a specific point located at a distance d1 from its rotational center. This lever incorporates a rack at its end, placed d2 units away from its rotational center. The rack interfaces with a pinion, which in turn is connected to a shaft. Parallel to the rack and pinion setup, the generator shaft is commonly associated with an inertia wheel (IW), and the pinion is connected to the shaft using a clutch bearing. Similar to the rack and pinion approach, this system also involves a spring to return the surface to its initial position. The efficiency of this type of system can extend to around 60% [9].

B. New mechanical system

For optimal generator shaft rotation, it's crucial to efficiently transmit the maximum force from the surface to the shaft, along with achieving the greatest possible displacement. In the rack and pinion mechanism, the transmitted force matches the force received on the surface, accounting only for the force absorbed by the spring. The angular displacement of the shaft corresponds to the linear surface displacement, divided by the pinion radius. Conversely, in the lever system, surface motion is magnified, but force is proportionally decreased, significantly diminishing the torque exerted on the generator shaft.

A more effective approach would involve optimizing both transmitted force and shaft rotation, with an emphasis on enhancing transmitted force. To achieve this objective, a system is proposed, utilizing a crank connected between the surface and a slider, as depicted in Figure 3. In this configuration, the crank length is denoted as "rcr," the height between crank axis as "hcr," the longitudinal distance between crank axis as "xcr," the crank angle as "0cr," the mechanical system piston longitudinal displacement as "xsp," the rack longitudinal displacement as "xra," the pinion angular displacement as "0p," and the IW angular displacement as "0iw."

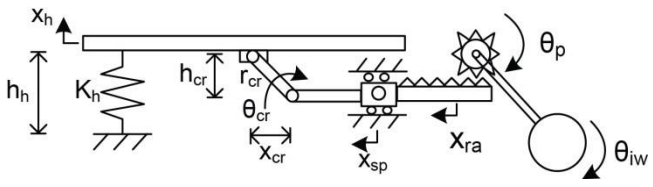

Fig. 3 Crank to slider system connected to a rack and pinion system and an IW.

This mechanism operates based on the subsequent fundamental concept: the surface undergoes linear displacement, initiating rotational motion in the crank, contingent on its length and initial angle. This crank, in sequence, impels the slider into translational motion, which is directly linked to a rack. Consequently, the rack triggers rotational motion in a pinion, which is then connected to both an inertia wheel (IW) and the electric generator shaft. The pinion's connection to the shaft employs a clutch bearing, with a spring incorporated to restore the surface to its initial position, functioning comparably to the springs in the lever or rack and pinion setups. Table IV provides a consolidated summary of all equations characterizing this system concerning kinematic, dynamic, and force analysis, for various motion scenarios: downward surface motion, surface halting, and upward surface motion. FSM1 denotes the force conveyed by the surface onto the mechanical system, while FSM1s signifies the countering force of the mechanical system on the surface. FSM2 represents the force transmitted from the crank to the slider piston, while FSM2s stands for the opposing force of the slider piston on the crank. The inertia of each component is symbolized as J, electric torque as ET, unidirectional bearing friction coefficient as bcb, electric generator friction coefficient as been, and mechanical piston friction-induced force losses as Flos.

CRANK TO SLIDER SYSTEM MODELLING USING A RACK AND PINION AND AN IW

Analysis	Downward motion	Upward motion
Kinematic	$x_{cr} = r_{cr}\,cos(\theta_{cr})$ $\theta_{cr} = sin^{-1}\left(\frac{h_{cr}}{r_{cr}}\right)$ $x_{sp} = x_{sp-in} - x_{cr}$ $h_{cr} = h_{cr-in} + x_h$ $x_r = x_{sp}$ $x_{ra} = r_p\,\theta_p \Leftrightarrow \theta_p = \frac{x_{ra}}{R_p}$ $\theta_{iw} = \theta_p$ $\theta_{iw} = \frac{x_{sp}}{r_p}$	$x_{cr} = r_{cr}\,cos(\theta_{cr})$ $\theta_{cr} = sin^{-1}\left(\frac{h_{cr}}{r_{cr}}\right)$ $x_{sp} = x_{sp-in} - x_{cr}$ $h_{cr} = h_{cr-in} + x_h$ $x_r = x_{sp}$ $x_{ra} = r_p\,\theta_p \Leftrightarrow \theta_p = \frac{x_{ra}}{r_p}$
Dynamic	$\ddot{x}_h = \frac{1}{m_h}[F_{SMs} + K_h x_h - F_v]$ $\ddot{x}_{sp} = \frac{1}{m_{sp}}[F_{SM2} - F_{SM2s} - F_{Los}]$ $\ddot{x}_r = \ddot{x}_{sp}$ $\ddot{\theta}_p = \ddot{\theta}_{iw} = \frac{(F_{SM2}\,r_p) - (b_{cb} + b_{gen})\dot{\theta}_p - ET}{J_p + J_{iw} + J_{gen}}$	$\ddot{x}_h = \frac{1}{m_h}[K_h x_h - F_{SMs}]$ $\ddot{x}_{sp} = \frac{1}{m_{sp}}[F_{SM2} - F_{SM2s} + F_{Los}]$ $\ddot{\theta}_p = -\frac{(F_{SM2}\,r_p) - (b_{cb}\dot{\theta}_p)}{J_p}$ $\ddot{\theta}_{iw} = \frac{-(b_{cb} + b_{gen})\,\dot{\theta}_{iw} - ET}{J_{iw} + J_{gen}}$
Forces	$F_{SM1} = F_v - K_h x_h$ $F_{SM2} = \frac{F_{SM1}}{tan(\theta_{cr})} - F_{Los}$ $F_{SM2s} = \frac{(J_p + J_{iw} + J_{gen})\,\ddot{\theta}_p + ET}{r_p}$ $F_{SMs} = F_{SM2s}\,tan(\theta_{cr})$	$F_{SM1} = -K_h.x_h$ $F_{SM2} = \frac{F_{SM1}}{tan(\theta_{cr})} + F_{Los}$ $F_{SM2s} = \frac{J_p\,\ddot{\theta}_p}{r_p}$ $F_{SMs} = F_{SM2s}\,tan(\theta_{cr})$

C. Energetic analysis: Given that the mechanical system yields linear output motion, the energy conveyed through the piston (ETr) is established according to equation (14). Equation (15) outlines the energy supplied from the inertia wheel (IW) to the electric generator (EDe). The effectiveness of the energy transmission system (ŋTr) is outlined in equation (16), establishing a connection between the energy conveyed and the energy garnered from the RPEH surface. Additionally, the efficiency of the energy delivery system (ŞDe) is formulated in equation (17), interrelating the energy furnished by the IW with the energy transmitted via the mechanical system.

$$\partial E_{Tr} = F_{SM2}\,\partial x_{sp} \quad (14)$$

$$E_{De} = (1/2) J_{iw} \dot{\theta}_{iw}^{\,2} \quad (15)$$

$$\eta_{Tr} = E_{Tr}/E_{Ha} \quad (16)$$

$$\eta_{De} = E_{De}/E_{Tr} \quad (17)$$

IV.ELECTRICAL SYSTEM: The simplest electrical configuration applicable to RPEH devices involves a purely direct current (DC) circuit design, featuring a DC electric generator, a DC resistive load exclusively, and a diode situated between the two components. Alternatively, in certain setups, a diode bridge is integrated. This arrangement is illustrated in Figure. 4

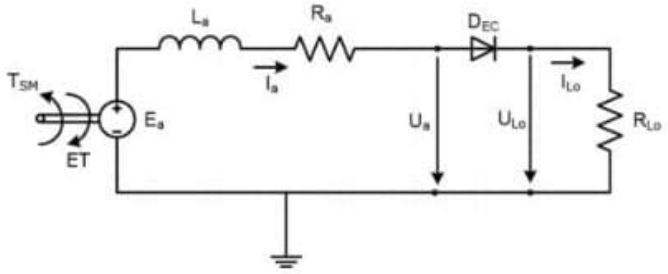

Fig. 4 Purely DC electric circuit with a DC electric generator and a resistive load. Models for both the permanent-magnet DC generator and the resistive load were developed based on key electric machine references, notably [18]-[20]. The mechanical torque of the system (TSM) initiates motion in the generator shaft, inducing a rotational velocity already defined by the IW speed (0iw). This process gives rise to an electromagnetic force (Ea), serving as the induced voltage across the generator armature. Through equation (18), the relationship between Ea and the generator shaft's rotational speed is established by multiplying it with the generator constant (ka). Equation (19) outlines the generated voltage (Ua) by considering factors like armature voltage (Ea), armature resistance (Ra), and armature current (Ia). For calculating the current within the armature windings, equation (20) is employed. It determines the armature current (Ia) based on elements such as armature inductance (La), armature resistance (Ra), circuit resistive load (RLo), generator constant (ka), and rotor angular speed (0iw). The electric torque (ET), opposing the mechanical system's movement, is quantified using equation (21).

$$E_a = k_a \dot{\theta}_{IW} \tag{18}$$

$$U_a = E_a - R_a I_a \tag{19}$$

$$\frac{di_a}{dt} = -\left(\frac{R_a + R_{Lo}}{L_a}\right) i_a + \left(\frac{k_a}{L_a}\right) \dot{\theta}_{IW} = \left(\frac{1}{L_a}\right)\left[k_a \dot{\theta}_{IW} - (R_a + R_{Lo}) I_a\right] \tag{20}$$

$$ET = I_a k_a \tag{21}$$

The inclusion of a diode between the electric generator and the electric load (DEC) establishes an electrical segregation between the two components. This configuration safeguards both elements, ensuring regulated voltage for the load and preventing reverse currents from affecting the generator armature. The electric load comprises solely of a resistive load, with an electric resistance (RLo) linked to both the diode and the electrical ground. The current supplied to the resistive load (ILo) mirrors the current generated by the generator (Ia), while the voltage supplied to the resistive load (ULo) is ascertained by equation (22), constrained by the voltage generated by the electric-generator.

$$U_{Lo} = I_{Lo} R_{Lo} \tag{22}$$

The power (PGe) and energy (EGe) produced by the DC electric generator are calculated using equations (23) and (24), respectively. Similarly, the power (PLo) and energy (ELo) consumed by a DC resistive load are computed using equations (25) and (26), respectively.

$$P_{Ge} = U_a I_a \tag{23}$$

$$E_{Ge} = \int P_{Ge}\, dt \tag{24}$$

$$P_{Lo} = U_{Lo} I_{Lo} \tag{25}$$

$$E_{Lo} = \int P_{Lo}\, dt \tag{26}$$

The efficiency of the energy transformation system (ȘGe) is outlined in equation (27), establishing a connection between the produced electric energy and the mechanical energy supplied by the IW. On the other hand, the efficiency of the electric circuit (ȘLo) is formulated in equation (28), linking the energy utilized by the electric load to the energy generated by the electric generator.

$$\eta_{Ge} = E_{Ge}/E_{De} \tag{27}$$

$$\eta_{Lo} = E_{Lo}/E_{Ge} \tag{28}$$

In order to compute the overall efficiency of the internal mechanism of the RPEH device (ȘRPEH), one should employ equation (29), establishing a correlation between the energy obtained by the mechanical system and the energy used by the electric-load.

$$\eta_{RPEH} = E_{Lo}/E_{Ha} \tag{29}$$

V. Technical Analysis

A. *Introduction*

A purely DC circuit that includes a DC electric generator, a DC entirely resistive electric load, and a diode between both is the most primitive electrical circuit to use in RPEH devices.

going circuits use a diode bridge

The design and development of the permanent-magnet DC generator and resistive load models followed the primary electric machine references, namely [18]–[20].

The generator shaft is actuated by the mechanical system torque (TSM) at a rotating speed that is already determined by the IW speed . This causes an electromagnetic force (Ea) to arise, which is the generator armature induced voltage.

By multiplying Ea by the generator constant (ka), equation (18) makes it possible to calculate Ea in relation to the rotational speed of the generator shaft. The produced voltage (Ua), in relation to the armature voltage (Ea), armature resistance (Ra), and armature current (Ia), is defined by equation (19). (20) must be utilized when calculating the current created in the armature windings, where the armature current (Ia) is related to the armature inductance.

The diode implemented between the electric generator and the electric load (DEC) establishes an electrical separation between both, protecting the two elements, guaranteeing a regulated voltage to the load while avoiding reversible current to the generator armature.

The electric load consists of a purely resistive load, using an electric resistance (RLo) connected to the diode and to the electric ground.

The current delivered to the resistive load (ILo)is the same as the current produced by the generator (Ia), while

After that, it calculates the different energies transferred from each part of the system to the others and the efficiency of each energy transfer process.

The simulations performed with Road VISS for the mechanical system presented in section 3 will be presented in this section.

The goal is to evaluate the new mechanical system and draw conclusions about its efficiency in transmitting and delivering mechanical energy.

One RPEH device connected to one mechanical system is considered, which, in turn, is connected to one electrical system, as the surface is actuated by one side of the vehicle.
So, the value presented for the energy lost by the vehicle is related to half the vehicle, as only one front and one rear wheel actuatesthe RPEH device surface.

The study focuses on the efficiency of the RPEH internal device (RPEH) in transmitting and delivering mechanical energy. The voltage delivered to the resistive load (ULo) is determined by the voltage produced by the electric generator. The power and energy generated by the DC electric generator are determined by (23) and (24), respectively. The total efficiency of the RPEH internal device (ȘRPEH) is determined by applying (29) to the total energy consumed by the electric load.

TABLE V
INPUT DATA FOR THE COMPUTATIONAL SIMULATIONS

Variable Name	Value	Unit
Vehicle class	Light	-
Vehicle weight	1,500	[kg]
Axles number | wheels/axle	2 | 2	-
Sprung-Unsprung %	90%-10%	-
Drag coefficient	0.32	-
Inertia moment	1,100	[kg.m^2]
Lift coef. (Front | Rear)	0.19 | 0.13	-
Motion | Direction	Free rolling | Forward	-
Vehicle speed | acceleration	40 | 0	[km/h] | [m/s^2]
Susp. type (F | R)	Indep. | Indep.	-
Susp. stiffness (F | R)	20,000 | 15,000	[N/m]
Susp. damping (F | R)	1,500 | 1,700	[Ns/m]
Tire type (F | R)	Radial | Radial	-
Tire stiffness (F | R)	150,000 | 150,000	[N/m]
Tire damping (F | R)	800 | 800	[Ns/m]
Tire pressure (F | R)	200 | 200	[kPa]
Tire ext diameter (F | R)	500 | 500	[mm]
Tire width (F | R)	200 | 200	[mm]
Tire tread width (F | R)	180 | 180	[mm]
Surface width	250	[mm]
Surface mass	20	[kg]
Surf max. height | max. disp	20 | 20	[mm]
Spring stiffness	40,000	[N/m]
Pinion mass | friction coef	1 | 0.002	[kg] | -
Inertia wheel radius	30	[mm]
EG constant Ka	0.25	-
EG Ra | La	1.1 | 0.0048	[Ɣ] | [H]
EG friction co. | Inertia	0.0008 | 0.05	-[kg.m^2]
Electric load Power	50	[W]

The parameters defined for the vehicle, the RPEH device surface, the mechanical and electrical systems, common in the simulations of the three mechanical systems are presented in Table V.

B. Simulation results

The authors used a software tool called RoadVISS to simulate the vehicle-road interaction from an energetic perspective. The software allows for detailed study of the interaction, including defining the vehicle's class, weight, axles, wheels, geometry, speed, acceleration, suspensions, tires, mechanical parameters, and the pavement or RPEH surface. The RPEH device's mechanical and electrical properties were also added to the model. The simulations performed with Road VISS for the mechanical system presented in section 3 aim to evaluate the new mechanical system and draw conclusions about its efficiency in transmitting and delivering mechanical energy. The energy lost by the vehicle is related to half the vehicle, as only one front and one rear wheel actuates the RPEH device surface.

The vehicle class is Light, with a weight of 1,500 kg, two axles, a spring-unsprung percentage of 90%-10%, a drag coefficient of 0.32, and an inertia moment of 1,100 kg. The vehicle's speed is free rolling, with an acceleration of 40 km/h. The suspension type is Radial, with a stiffness of 20,000-15,000 N/m and a damping of 1,500-1,700 Ns/m. The tire type is Radial, with a stiffness of 150,000 N/m and a damping of 800 Ns/m. The tire pressure is 200 kPa, and the tire dimensions are 500 mm in diameter, 200 mm in width, 180 mm in tread width, and 250 mm in surface width. The surface mass is 20 kg, and the surface max. height is 20 mm. The spring stiffness is 40,000 N/m, and the pinion mass has a friction coefficient of 0.002 kg. The EG constant is 0.25, and the EG friction coefficient is 0.0008 kg. The electric load power is 50 W.

TABLE VI
SIMULATION RESULTS FOR THE ENERGY OUTPUTS OF THE RPEH DEVICE COMPONENTS USING THE CRANK TO SLIDER MECHANICAL SYSTEM

r_{cr} [mm]	r_p [mm]	m_{iw} [kg]	E_v [J]	E_{Ha} [J]	E_{Tr} [J]	E_{De} [J]	E_{Ge} [J]	E_{Lo} [J]
35	15	5	224	91	23	23	20	16
		10	224	91	23	23	19	15
	20	5	222	89	42	42	38	31
		10	222	89	42	42	36	29
	25	5	221	87	65	65	58	48
		10	221	87	65	65	54	43
40	15	5	222	88	38	38	33	27
		10	222	88	38	38	32	26
	20	5	219	85	67	67	60	49
		10	219	85	67	67	55	45

25	5	218	83	82	82	75	61
	10	218	83	82	82	73	60

TABLE VII
SIMULATION RESULTS FOR THE EFFICIENCIES OF THE RPEH DEVICE COMPONENTS USING THE CRANK TO SLIDER MECHANICAL SYSTEM

r_{cr} [mm]	r_p [mm]	m_{iw} [kg]	η_{Ha} [%]	η_{Tr} [%]	η_{De} [%]	η_{Ge} [%]	η_{Co} [%]	η_{RPEH} [%]
35	15	5	40.6	25.3	99.5	87.2	80.2	17.6
		10	40.6	25.3	99.5	86.6	79.8	17.4
	20	5	40.1	47.2	99.5	90.5	81.7	34.9
		10	40.1	47.2	99.5	87.7	80.5	33.3
	25	5	39.4	74.7	99.5	90.3	81.8	55.1
		10	39.4	74.7	99.5	83.1	81.2	50.4
40	15	5	39.6	43.2	99.5	89.2	81.4	31.3
		10	39.6	43.2	99.5	86.3	80.5	30.0
	20	5	38.8	78.8	99.5	90.4	81.7	58.2
		10	38.8	78.8	99.5	83.3	81.2	53.3
	25	5	38.1	98.8	99.5	91.9	81.9	74.3
		10	38.1	98.8	99.5	90.1	81.5	72.5

Simulation results Considering the input data presented in Table V, simulations for the crank to slider mechanical system were performed and the main results are presented in Tables VI and VII for the energy output and the efficiency of each component of the system, respectively. The crank length, pinion radius and IW mass were changed between simulations to evaluate the impact of these variables in the system's performance

VI. DISCUSSION

Analyzing the results obtained with the computational simulations of the RPEH device, using the mechanical system developed to transmit the energy received by the equipment surface and deliver it to an electrical generator, some conclusions may be drawn.

The mechanical energy transmission efficiency is greatly affected by the crank length and pinion radius values, varying from 25% to 99% with the simulated values.

The mechanical energy delivery efficiency is close to 100%, meaning that the IW delivers almost all the energy that the pinion transmits to it.

Comparing the different parameters of the mechanical systems for the same conditions, it may be concluded that: x an increase in the pinion radius induces an increase in the energy transmission efficiency.

VII. CONCLUSION

In locations where cars must release energy to the pavement in order to slow down, the idea of road pavement energy harvesting has gained popularity in recent years. Its goal is to transform the mechanical energy of moving automobiles into electrical energy.

In order to transfer the mechanical energy that the equipment's surface receives to an electrical generator, which transforms the mechanical energy into electrical energy, certain technologies have been created recently, most of which use mechanical systems.

The mechanical energy is delivered and stored by an IW that is connected to the shaft of the electrical generator in electromechanical systems that have been created thus far. These systems primarily use the rack and pinion and lever systems.

In this study endeavor, a new mechanical mechanism was designed to transfer and distribute the mechanical energy acquired by the RPEH surface to an electrical generator.

The system's physical models were established.

In order to maximize the amount of energy transferred from the mechanical system to the electrical generator, the created method—described as a crank to slider system—aims to increase the force applied by the vehicle in the RPEH device surface.

The mechanical system and the remainder of the RPEH device were modelled, and computational simulations were run to determine the amounts of energy harvested, transmitted, delivered, converted, and consumed by the RPEH device. This was done using software that the authors had previously developed [21] to simulate the vehicle-road interaction.

After analyzing the data and taking into account the best case scenarios shown in [9], it can be said that the new mechanical system that has been suggested is more efficient than the rack and pinion and lever systems.

Its primary benefit is an increase in transmitted force, which results in a higher mechanical energy transmission. This means that the pinion and, by extension, the IW and the generator shaft, accelerate more quickly, increasing rotation speed and the amount of energy delivered, converted, and transmitted.

The next phase of this research project will involve creating a prototype so that the proposed system can be tested in a lab setting and experimental outcomes may be obtained.

These will enable us to draw judgments regarding the system's technical viability when compared to the theoretical outcomes produced by the computational simulations.

ACKNOWLEDGMENT

I would like to express my profound gratitude in completing this research paper, made possible through the invaluable support and guidance provided by my college. The institution's commitment to academic excellence and its conducive environment fostered an atmosphere where intellectual curiosity could thrive. The dedicated faculty not only imparted knowledge but also nurtured critical thinking, pushing me to explore new horizons in my research. Additionally, the resources and facilities extended by the college played a pivotal role in the accomplishment of this work. This research journey has been enriched by my college's unwavering encouragement, contributing significantly to my academic growth.

REFERENCES

[1] IEA, *Special Report on Energy and Climate Change*, International Energy Agency, Paris, France (2015). See: https://www.iea.org/publications/freepublications/publication/WEO2015SpecialReportonEnergyandClimateChange.pdf

[2] IEA, *Special Report on Energy and Air Pollution*, International Energy Agency, Paris, France (2016). See: http://www.iea.org/publications/freepublications/publication/WorldEnergyOutlookSpecialReport2016EnergyandAirPollution.pdf

[3] Khaligh, A. and Onar, O.C., *Energy harvesting: solar, wind, and ocean energy conversion systems*. CRC Press Inc, Boca Raton, FL, USA (2010).

[4] Priya, S. and Inman, D.J. (eds.), *Energy harvesting technologies*, vol. 21. Springer, New York, NY, USA (2009).

[5] Kazmierski, T. and Beeby, S. (eds.), *Energy harvesting Systems - Principles, Modeling and Applications*. Springer, New York, NY, USA (2009).

[6] Harb, A., "Energy Harvesting: State-of-the-art," *Renewable Energy*, 36(10): 2641-2654 (2010).

[7] Yildiz, F., "Potential ambient energy-harvesting sources and techniques," *The Journal of Technology Studies*. 35(35): 40-48 (2009).

[8] Andriopoulou, S., *A review on energy harvesting from roads*. KTH, Stockholm, Sweden (2012).

[9] Duarte, F. and Ferreira, A., "Energy harvesting on road pavements: state of the art," *Proceedings of Institution of Civil Engineers - Energy*, 169(2): 79-90 (2016).

[10] IEA, *Technology Roadmap: Fuel Economy of Road Vehicles*. International Energy Agency, Paris, France (2012). See: http://www.iea.org/publications/freepublications/publication/Fuel_Economy_2012_WEB.pdf.

[11] Hendrowati, W., Guntur, H.L. and Sutantra, I.N., "Design, modelling and analysis of implementing a multilayer piezoelectric vibration energy harvesting mechanism in the vehicle suspension," *Engineering*, 4(11): 728-738 (2012).

[12] Gillespie, T., *Fundamentals of vehicle dynamics*. Society of Automotive Engineers, Warrendale, PA, USA (1992).

[13] Wong, J., *Theory of ground vehicles*. *3rd Edition*. Wiley, New York, NY, USA (2001).

[14] Blundell, M. and Harty, D., *Multibody systems approach to vehicle dynamics*. Elsevier Butterworth-Heinemann, Oxford, UK (2004).

[15] Jazar, R., *Vehicle dynamics: theory and application*. Springer, New York, NY, USA (2008).

[16] 3RSS.6FKLHKOHQ:.UR JHU0DQG3DQQLQJ/*Ground vehicle dynamics*. Springer, Berlin, Germany (2010).

[17] Rajamani, R., *Vehicle dynamics and control*. Springer, New York, NY, USA (2011).

[18] Chapman, S., *Electric Machines Fundamentals, Fourth Edition*. McGraw-Hill, New York, NY, USA (2004).

[19] Lyshevski, S., *Electromechanical Systems and devices*. CRC Press Inc, Boca Raton, FL, USA (2008).

[20] Murthy, K., *Computer-aided design of electrical machines*. BS Publications, Hyderabad, India (2008).

[21] Duarte, F., Ferreira, A. and Fael, P., "Software for simulation of vehicleroad interaction," In: *New Advances in Information Systems and Technologies*, Vol. 444 of the *Series Advances in Intelligent Systems*..